Observations of ion cyclotron waves in the solar wind near 0.3 AU

L. K. Jian,[1] C. T. Russell,[1] J. G. Luhmann,[2] B. J. Anderson,[3] S. A. Boardsen,[4,5] R. J. Strangeway,[1] M. M. Cowee,[6] and A. Wennmacher[7]

Received 30 May 2010; revised 3 September 2010; accepted 13 October 2010; published 31 December 2010.

[1] Using 2 Hz magnetic field data from the MESSENGER mission, we have investigated more than 300 strong narrowband ion cyclotron wave (ICW) events at a heliocentric distance of about 0.3 AU during 31 May to 9 June 2008. These nearly circularly polarized transverse waves are observed extensively and discretely in the solar wind, with a median duration of 21 s. They are preferentially observed when the magnetic field is more radial than the ambient solar wind. The waves appear both left-handed and right-handed in the spacecraft frame. Their wave frequencies in the spacecraft frame are generally larger than the local proton cyclotron frequency (f_{pc}), with a median of 1.44 f_{pc}. The wave power spectra do not cutoff at the local f_{pc}. On the basis of their wave characteristics, we conclude that they are intrinsically left-handed in the solar wind frame and they are generated closer to the Sun and carried out to the spacecraft by the super Alfvénic solar wind. After removing the Doppler shift, the wave frequencies in the solar wind frame are all below the local f_{pc}, with a median of 0.35 f_{pc}. The ICWs propagate nearly parallel to the magnetic field, and the median wave amplitude is about 0.73 nT, 3% of the background magnetic field. We compare these observations with earlier Helios observations at 0.3 AU in 1976 and contemporary 1 AU observations.

Citation: Jian, L. K., C. T. Russell, J. G. Luhmann, B. J. Anderson, S. A. Boardsen, R. J. Strangeway, M. M. Cowee, and A. Wennmacher (2010), Observations of ion cyclotron waves in the solar wind near 0.3 AU, *J. Geophys. Res.*, *115*, A12115, doi:10.1029/2010JA015737.

1. Introduction

[2] Ion cyclotron waves (ICWs) are left-handed (LH) circularly polarized waves at frequencies below but in the vicinity of the cyclotron frequency of the dominant ion in the plasma frame. ICWs are on the same wave "branch" but are different from Alfvén waves, which occur well below the ion cyclotron frequency and hence do not resonantly interact with the gyromotion of the ions. Alfvén waves are linearly polarized waves and can be treated in the MHD approximation. ICWs can be generated by perpendicular pickup ions, which are produced by photoionization or charge exchange and then accelerated by the electric field of a magnetized plasma flowing through the neutral gas. ICWs have been observed in a variety of planetary and cometary environments [e.g., *Fraser*, 1985; *Neubauer et al.*, 1993; *Huddleston et al.*, 1998; *Leisner et al.*, 2006; *Russell and Blanco-Cano*, 2007], but only occasionally reported to be seen in the solar wind.

[3] Using ion spectrometers, *Möbius et al.* [1985], *Gloeckler et al.* [1993], and *Geiss et al.* [1994] directly detected the interstellar pickup He^+, H^+, as well as O^+, N^+, and Ne^+ in the solar wind, respectively. Theoretical studies on the pickup in the interplanetary space began long before such discoveries. *Wu and Davidson* [1972] first discussed the growth rates for both parallel (where magnetic field and solar wind velocity are parallel) and perpendicular pickup geometries, with the specification for He^+ addressed by *Wu et al.* [1973]. *Lee and Ip* [1987] studied the time-dependent behavior of the pickup ion velocity distribution and the generated wave spectrum. *Williams and Zank* [1994] analyzed the wave polarization for parallel and perpendicular geometry with some discussion of the growth rates as well. *Isenberg* [1996] showed the relative intensities for LH and right-handed (RH) waves in the parallel case.

[4] Briefly, these studies suggested that perpendicular pickup ions produce ICWs that are LH polarized and near the ion cyclotron frequency in the plasma frame. When the magnetic field is more aligned with the flow, the pickup ions have a large parallel drift velocity relative to the solar wind and will generate waves that are RH polarized in the plasma

[1]Institute of Geophysics and Planetary Physics, University of California, Los Angeles, California, USA.
[2]Space Science Laboratory, University of California, Berkeley, California, USA.
[3]Applied Physics Laboratory, Johns Hopkins University, Baltimore, Maryland, USA.
[4]Heliophysics Science Division, NASA Goddard Space Flight Center, Greenbelt, Maryland, USA.
[5]Goddard Earth Sciences and Technology Center, University of Maryland, Baltimore, Maryland, USA.
[6]Space Science and Applications (ISR-1), Los Alamos National Laboratory, Los Alamos, New Mexico, USA.
[7]Institute of Geophysics and Meteorology, University of Cologne, Cologne, Germany.

Copyright 2010 by the American Geophysical Union.
0148-0227/10/2010JA015737

frame and propagating toward the Sun. In the spacecraft frame, the polarization of these waves generated by the field-aligned beams of parallel pickup ions can be reversed and appear LH polarized because the solar wind speed is faster than the radial wave speed (approximated using the Alfvén speed V_A). In these two limits of perpendicular and parallel pickup, the waves appear just below and just above the local ion cyclotron frequency in the spacecraft frame, which is nearly static with respect to the frame of the neutrals.

[5] Consistent with theory, *Murphy et al.* [1995] found the waves accompanying the pickup of interstellar hydrogen from 4.6 to 5.4 AU using Ulysses magnetic field data. The waves are LH in the spacecraft frame and exhibit a cutoff in the wave spectra at the local proton cyclotron frequency (f_{pc}). Since the interplanetary magnetic field (IMF) was nearly aligned with the solar wind during these events, the observed LH polarization in the spacecraft frame is consistent with the expected RH polarization in the plasma frame for parallel pickup generation. In addition, the lower-frequency cutoff of the wave spectrum was at the local f_{pc}, as expected for the pickup of interstellar neutral hydrogen. *Murphy et al.* [1995] found only 31 wave events over 640 days. The waves typically lasted 1 h or more.

[6] In contrast, *Jian et al.* [2009] reported ICWs with quite different properties at 1 AU using 8 Hz magnetic field data from STEREO (Solar Terrestrial Relations Observatory) mission. The waves appear both LH and RH polarized in the spacecraft frame. The wave properties of the LH and RH waves are similar despite the different apparent handedness. The wave spectra were not cutoff at the local f_{pc}. The waves occurred in bursts (occasionally continuously) with a median duration of only 51.5 s and 246 events were found over 16 days, much more often than the waves of *Murphy et al.* [1995]. In addition, the median wave amplitudes relative to the background magnetic field differ by a factor of 12, being about 0.36 for the waves of *Murphy et al.* [1995] near 5 AU and 0.03 for the waves found by *Jian et al.* [2009] at 1 AU. This is consistent with the theoretical work suggesting that parallel pickup generates waves of larger amplitude than the perpendicular pickup. However, the ICWs of *Jian et al.* [2009] are not likely due to local perpendicular pickup, because they are seen more preferentially when the IMF is radial than perpendicular and they are not at the local proton or helium cyclotron frequency. It is also possible that none of the aforementioned theoretical work treated the intermediate field geometry self-consistently. In this paper, we investigate the ICWs near 0.3 AU, the closest distance any spacecraft have ever been to the Sun, to determine if these ICWs have properties similar to those near 1 AU and to provide constraints on the possible generation mechanisms of these waves.

2. Observations Using MESSENGER Magnetometer Data

[7] MESSENGER (Mercury Surface, Space Environment, Geochemistry, and Ranging) mission is scheduled to enter Mercury orbit in March 2011 [*Domingue and Russell*, 2007]. Since its launch on 3 August 2004, the MESSENGER spacecraft has already completed two Venus flybys and three Mercury flybys. Its trajectory between these encounters provides an opportunity to explore the solar wind in the inner heliosphere. While MESSENGER does not have the in situ measurements of the solar wind per se, it does provide 2 Hz magnetometer data for much of its interplanetary travel time, with a digital noise level at 2 Hz of about 2.5×10^{-4} nT^2/Hz [*Anderson et al.*, 2007] that allows sensitive measurements of ICWs.

[8] We choose a 10 day period, 31 May to 9 June in 2008, to explore the ICWs in the regions closest to the Sun, i.e., near 0.3 AU. The selection of this 10 day period is based on three factors. First, 2008 is in the middle of the quiet solar minimum 23/24, a similar time window as our previous STEREO observations. Second, from the MESSENGER magnetic field data, we do not see any interplanetary coronal mass ejections or interplanetary shocks during this interval. Third, the spacecraft was more than 0.13 AU (about 7971 Mercury radii and 3214 Venus radii) away from Mercury and Venus, so we can exclude planetary influences.

[9] On the basis of a visual inspection of the 2 Hz magnetic field data, we choose candidate intervals to conduct quadrature spectrum analysis. The quadrature power spectral matrix is the variance matrix of the out-of-phase cross powers, and the cospectral matrix is the variance matrix of the in-phase power. The in-phase power can be analyzed in a manner totally analogous to the minimum variance or principal axis analysis to get a direction of propagation but does not return handedness. *Means* [1972] found that the quadrature spectral matrix which is antisymmetric with a zero trace has the direction of propagation in the three upper right (or equivalently the three lower left) matrix elements. These elements of the matrix are composed of all circularly polarized power and have handedness information because these out-of-phase components can be 90° ahead or behind. Thus, this direction of propagation has a sign and can be used to distinguish LH and RH waves. See *Means* [1972] for detail. Such a wave analysis program has been in use at UCLA for almost 30 years and has been used in hundreds of applications. It has also been tested against simulated waves with known handedness such as lightning generated whistler waves in a non-Doppler shifting environment.

[10] After the wave analysis of candidate time intervals, we select ICWs in the solar wind based on the following three criteria. First, the transverse power is dominant as expected for an ICW; second, the absolute value of ellipticity is larger than 0.7, meaning that the wave is nearly circularly polarized; third, the percentage of polarization is larger than 70%, indicating that the signal-to-noise ratio is high. Each of the waves selected using the above three criteria is observed to have the long axis of its perturbation ellipse within 10° of the direction perpendicular to both magnetic field ($\boldsymbol{B}$) and wave propagation direction ($\boldsymbol{k}$) no matter whether $\boldsymbol{k}$ is from the principal axis analysis or Means technique, i.e., the long axis nearly perpendicular to the $\boldsymbol{B}$-$\boldsymbol{k}$ plane. This observation indicates these waves are intrinsically LH in the plasma frame, because the long axis of the perturbation ellipse would be in the $\boldsymbol{B}$-$\boldsymbol{k}$ plane for RH waves [*Stix*, 1962; *Lacombe et al.*, 1990; *Blanco-Cano*, 1995].

[11] During the 10 day survey, we detected 308 wave events. Their duration varies from 8.5 to 194 s, with a median of 21 s. They cumulatively are present 0.94% of the 10 days. The power spectra of 26 wave events have more than one

peak (one event with three peaks), and these peaks are comparable to each other; we count each peak as one event. In total, there are 335 wave events. While these waves appear both LH and RH with respect to the background field in the spacecraft frame, most of the waves (72% or 240 events) are LH polarized (negative ellipticity) in the spacecraft frame. Figure 1 displays the ellipticity and location of the ICW events in the context of the IMF strength and direction. The waves do not concentrate within the heliospheric plasma sheet bounded by a pair of gray dashed vertical lines in Figure 1. We note, although both LH and RH waves in the spacecraft frame can be observed nearby, one handedness predominates at any time. In addition, there are several time intervals when a large number of wave events were gathered in close proximity, for instance, at 1700–2200 UT of 3 June 2008, and also the time period shown in Figure 2a.

[12] Figure 2 illustrates an example of these ICWs. There are a series of wave events within the 30 min window of Figure 2a. The time variations and power spectrum of the magnetic field for the wave of the interval T1–T2 are displayed in Figures 2b and 2e. From the wave analysis, the wave is found to be RH in the spacecraft frame. The ellipticity is 0.96, and the percentage of polarization is 98%, so the wave is a circularly polarized wave. It propagates only 1° away from the magnetic field. Transforming the magnetic field from the RTN coordinate to the minimum variance coordinates as shown in Figure 2d, we can see the minimum variance direction $\boldsymbol{K}$ is nearly antiparallel to the magnetic field. From the hodogram in Figure 2e, we can see the wave is LH circular with respect to $\boldsymbol{K}$ and therefore RH circular with respect to the field direction. The handedness from the hodogram is the same as that obtained directly from the wave analysis program. Since the solar wind speed is much greater than the phase speed of these ICWs (approximated by V_A), waves that are propagating inward toward the Sun will be carried outward over the spacecraft and the observer will see these waves "unwound" by the Doppler shift. Thus, inward moving waves appear to be RH polarized in the spacecraft frame.

[13] In Figure 1, we note the ICWs tend to be observed when the field is radial, regardless of whether it is radially inward or radially outward. We further compare the distributions of the angle between the IMF and the radial direction ($\boldsymbol{B}$-$\boldsymbol{R}$ angle) for the ICWs and for the whole 10 days, as displayed in Figure 3a. While the IMF direction is distributed broadly, mostly 20°–45° away from the radial direction, the $\boldsymbol{B}$-$\boldsymbol{R}$ angle for ICWs is indeed smaller than that for the nominal solar wind. This trend is shown more clearly in Figure 3c when we normalize the distribution of $\boldsymbol{B}$-$\boldsymbol{R}$ angle for ICWs by the 10 day distribution. In Figure 3b, we cannot see any clear dependence of the wave power on the $\boldsymbol{B}$-$\boldsymbol{R}$ angle. This cannot help distinguish parallel or perpendicular pickup, but it supports the scenario that the waves are not locally generated, because if the waves are locally generated, the wave power will be highest for small $\boldsymbol{B}$-$\boldsymbol{R}$ angle (parallel pickup) or large $\boldsymbol{B}$-$\boldsymbol{R}$ angle (perpendicular pickup).

[14] In addition, we have analyzed the propagation angle of the ICWs with respect to the magnetic field. The angle varies from 0.1° to 17.6°, with a median of 4°. Figure 3d indicates the wave power decreases monotonically with the increase of propagation angle. To determine whether this is due to the variation of growth rate with the propagation angle, the theory for the intermediate-pickup geometry needs to develop. On the other hand, the decrease in power is consistent with the fact that ICWs are damped more if they propagate obliquely to the magnetic field direction. Normalizing the propagation angle distribution by the solid angle subtended by each bin as shown in Figure 3e, we can see that the propagation vector of these waves is very close to the field direction.

[15] Because the waves are intrinsically LH in the plasma frame and they will always be carried outward by the solar wind, we conclude that both the LH and RH waves are generated closer to the Sun than the spacecraft, i.e., within 0.3 AU. Using the same Doppler shift relation of *Jian et al.* [2009], we can convert the weighted frequency (averaged with a weight of power) in the spacecraft frame (f_{sc}) to the one in the solar wind frame (f_{sw}),

$$f_{sw} = f_{sc} - \frac{\boldsymbol{k}\cdot\boldsymbol{V}_{sw}}{2\pi} = f_{sc}\Big/\left(1 + \frac{V_{sw}}{V_A}\hat{\boldsymbol{k}}\cdot\hat{\boldsymbol{V}}_{sw}\right), \qquad (1)$$

where $\boldsymbol{k}$ is the wave propagation vector and $\boldsymbol{V}_{sw}$ is the solar wind velocity relative to the spacecraft. Because V_{sw} is usually 5–8 times V_A and waves mostly propagate close to the radial solar wind direction, the Doppler shift term dominates. From the handedness in the spacecraft frame, we can determine whether the waves propagate sunward (RH in spacecraft frame) or antisunward (LH in spacecraft frame) in the solar wind frame and then obtain f_{sw}. Because MESSENGER mission does not measure the solar wind plasma, we assume a constant solar wind speed of 360 km/s and a constant proton number density of 39 cm^{-3} for this 10 day period, based on the solar wind parameters measured at 1 AU for the corresponding time window and the conservation of solar wind flux. The values are about right for the unusual solar minimum 23/24 with slower solar wind and smaller proton number density than usual.

[16] In Figure 4, we compare the wave parameters of LH and RH waves in the spacecraft frame using the paired histograms. The LH waves are generally stronger, with a median power 3 times that of the RH waves. Consistent with the lower power of RH waves, only 28% of the waves we detected are RH polarized in the spacecraft frame. LH and RH waves in the spacecraft frame have similar propagation angles from $\boldsymbol{B}$ as shown in Figure 4b. The median f_{sc} of LH waves is 0.6 Hz, 20% higher than the f_{sc} of RH waves. This agrees with a higher f_{sc} of LH waves than RH waves obtained at 1 AU [*Jian et al.*, 2009]. If the waves were generated in the same rest frame as the spacecraft, the initial frequency should be the same as the measured f_{sc}. So the higher f_{sc} of LH waves could be because they are generated in regions closer to the Sun than the RH waves, where the field is stronger. This is also consistent with our scenario that LH waves have faster travel speed (approximated by $V_A + V_{sw}$) so that they can survive to a longer distance than RH waves. Overall, about 90% of these waves have the f_{sc} larger than the local f_{pc}, which is the highest cyclotron frequency of various ions, again suggesting these waves are unlikely to be generated locally by pickup ions.

[17] After removing the Doppler shift, the median f_{sw} of LH waves is about 0.14 Hz, 22% lower than the median of the RH waves. Nearly all the f_{sw} are smaller than the local f_{pc},

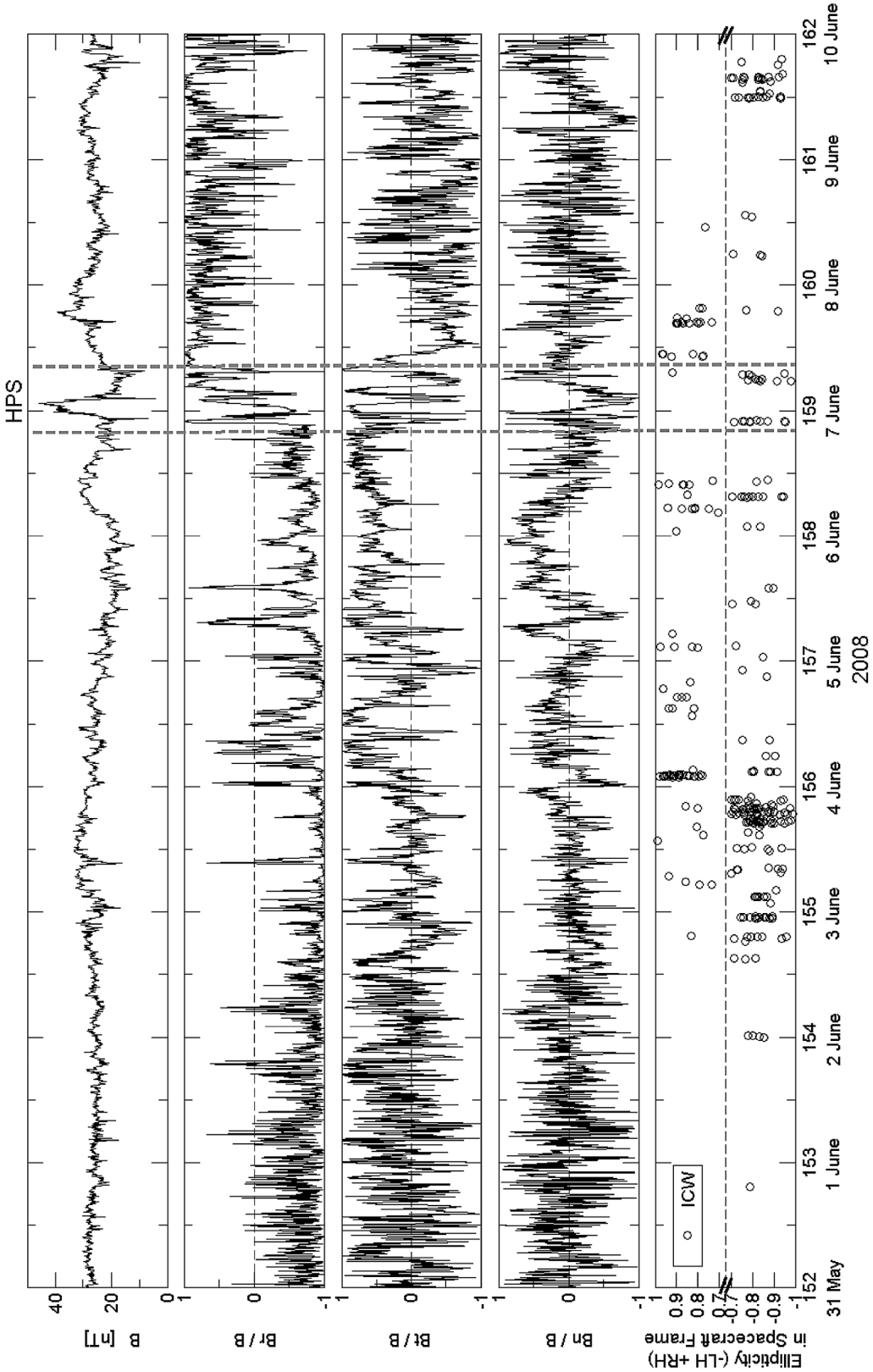

Figure 1. Occurrence of ICWs observed by MESSENGER during 31 May to 9 June 2008. (from top to bottom) Magnetic field intensity, ratios of the magnetic field components in radial-tangential-normal (RTN) coordinates to the total field intensity, ellipticity of ICWs in spacecraft frame marked by circles. In the RTN coordinates, ***R*** points away from the Sun center to the spacecraft, ***N*** is the projection of the solar rotational axis on the plane of the sky, and ***T*** is formed by the cross product of ***N*** and ***R*** and lies in the solar equatorial plane. The displayed magnetic field data are of 5 min resolution. The region bounded by a pair of gray dashed vertical lines is the heliospheric plasma sheet (HPS) surrounding the heliospheric current sheet.

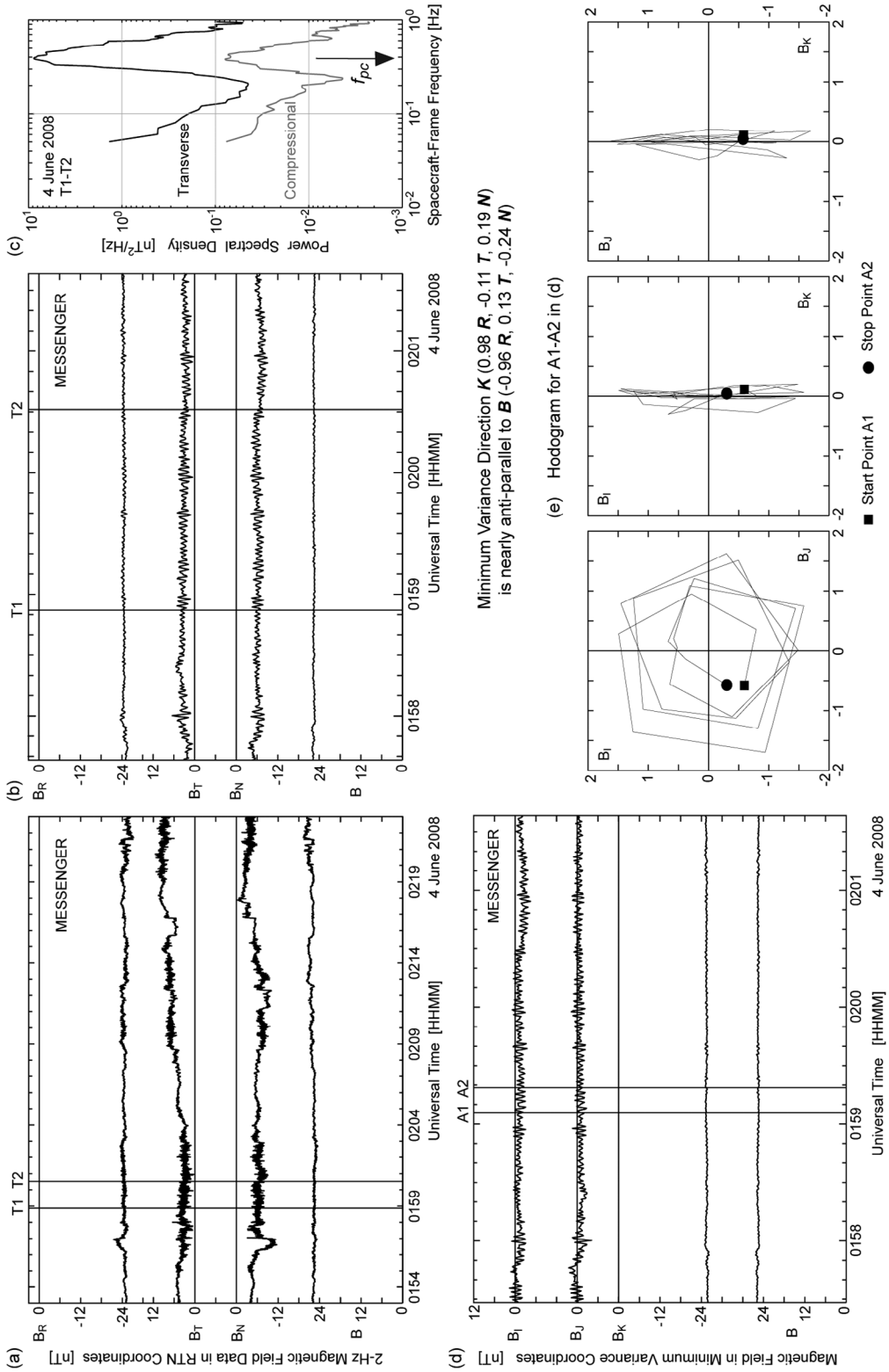

Figure 2. Example of an ICW observed on 4 June 2008 by MESSENGER. (a) Time series of 2 Hz magnetic field vector for 30 min in RTN coordinates. (b) Magnetic field vector for 4 min in RTN coordinates. (c) Power spectrum of the wave during the interval T1–T2 marked in Figures 2a and 2b, averaged using nine frequency bands. The transverse power is 2 orders of magnitude stronger than the compressional power. (d) Magnetic field in the minimum variance coordinates, where the unit vectors ***I***, ***J***, ***K*** define a right-handed coordinate system where ***I*** is in the maximum variance direction, ***J*** is in the intermediate, and ***K*** is in the minimum variance direction. The wave propagation direction is indicated by the ***K*** direction, which is nearly antiparallel to the magnetic field ***B*** for this event. (e) Hodogram for the magnetic field in the minimum variance coordinates during the time interval A1–A2 marked in Figure 2d. In the first box, the ***K*** direction points into the paper, opposite to ***B***. So that the wave is RH circularly polarized around ***B***.

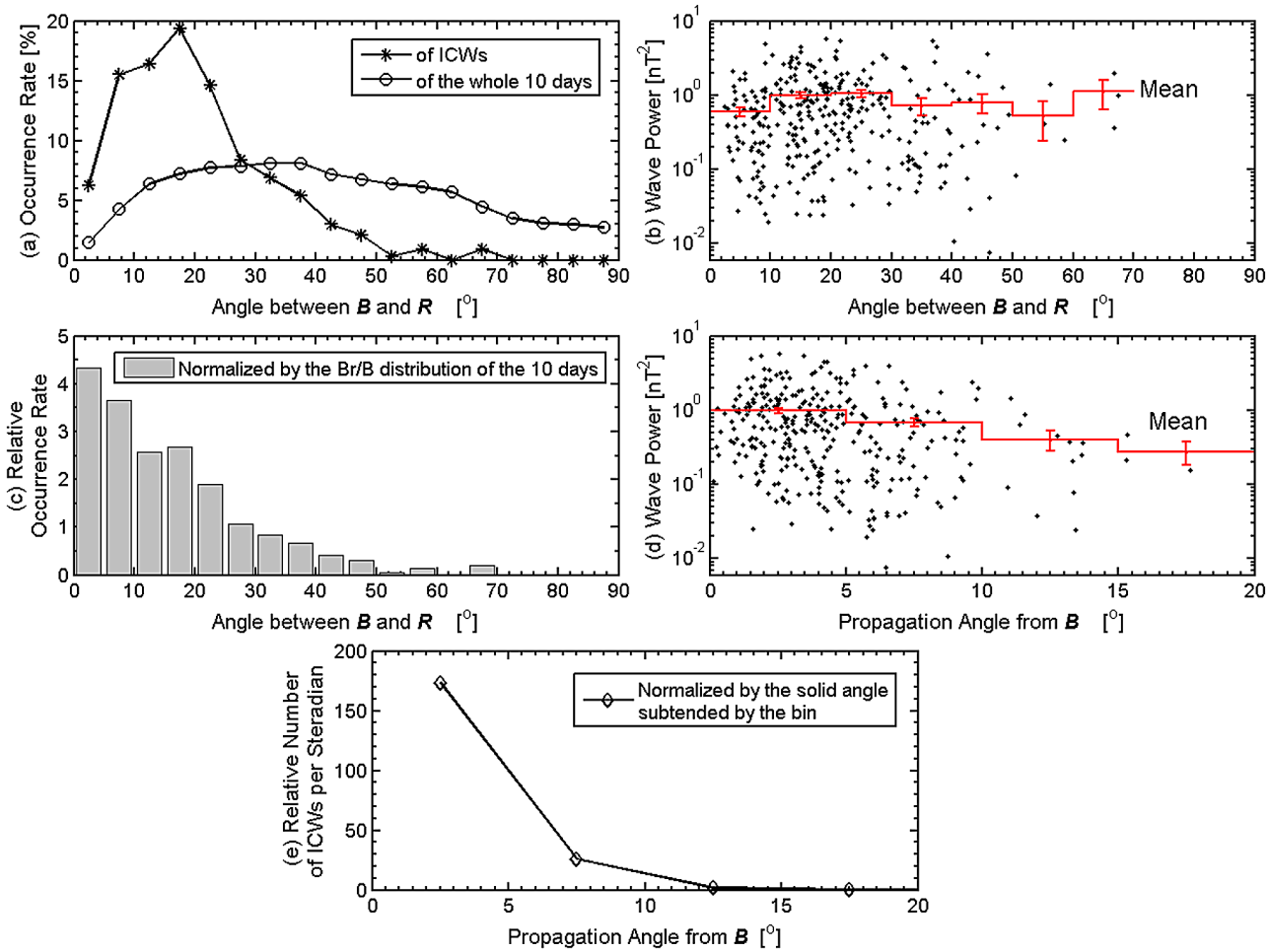

Figure 3. (a) The distributions of the angle between magnetic field and radial direction (***B***-***R*** angle) for ICWs (marked by asterisk) and for the whole 10 days (marked by circle), where 20 s averaged field data are used for the 10 day distribution to match the typical duration of ICWs. (b) The scatterplot of the wave power versus the ***B***-***R*** angle, where the stepwise line indicates the mean value for each angular bin and the error bar denotes the probable error of the mean (the standard deviation divided by the square root of the event count). (c) The distribution of the ***B***-***R*** angle during ICWs normalized by the ***B***-***R*** angle distribution for the whole 10 days. (d) The scatterplot of the wave power versus the ***B***-***R*** angle, where the stepwise line indicates the mean value for each bin and the error bar denotes the probable error of the mean. (e) The distribution of wave propagation angle from ***B*** obtained through principal axis analysis, normalized by the solid angle subtended by the bin. Because the largest propagation angle is smaller than 20°, the scales of the abscissa axis in Figures 3d and 3e are 0°–20°, different from other panels.

consistent with the fact that waves approaching the f_{pc} will be resonantly damped by local solar wind protons [e.g., *Li et al.*, 1999; *Tu and Marsch*, 2001]. After normalizing the f_{sc} and f_{sw} by the local f_{pc}, the shapes of the histogram distributions do not change dramatically. Comparing the f_{sw} and f_{sc} for LH waves, we can clearly see the Doppler shift conversion has changed the histogram distribution. In contrast with RH waves, the distributions of f_{sw} and f_{sw}/f_{pc} are both narrower for LH waves. For the f_{sw} of LH waves, there seem to be an upper limit at about 0.5 f_{pc} (the cyclotron frequency of He^{2+}) and a median at about 0.3 f_{pc} (around the cyclotron frequency of He^{+}). But for the f_{sw} of RH waves, the upper limit is at about f_{pc} and the median is at about 0.4 f_{pc}. Whether the He^{2+}, He^{+}, or other ions have any correlation with the ICWs needs further investigation using the frequency band rather than a single weighted frequency for each individual wave event. We plan to explore it in future studies.

3. Observations Using Helios 1 Measurements

[18] We have surveyed ICWs near 0.3 AU, not only using MESSENGER measurements, but also using Helios 1 observations. Helios 1 provided 4 Hz magnetometer data [*Neubauer et al.*, 1977] for limited time periods. We chose 25–31 March 1976 to investigate, because Helios 1 was near its perihelion and 1976 is in the middle of solar minimum 20/21 and three solar cycles ahead of MESSENGER observations, which were obtained during solar minimum too. An example of ICWs from Helios 1 observations is illustrated in Figure 5. In the spacecraft frame, the wave

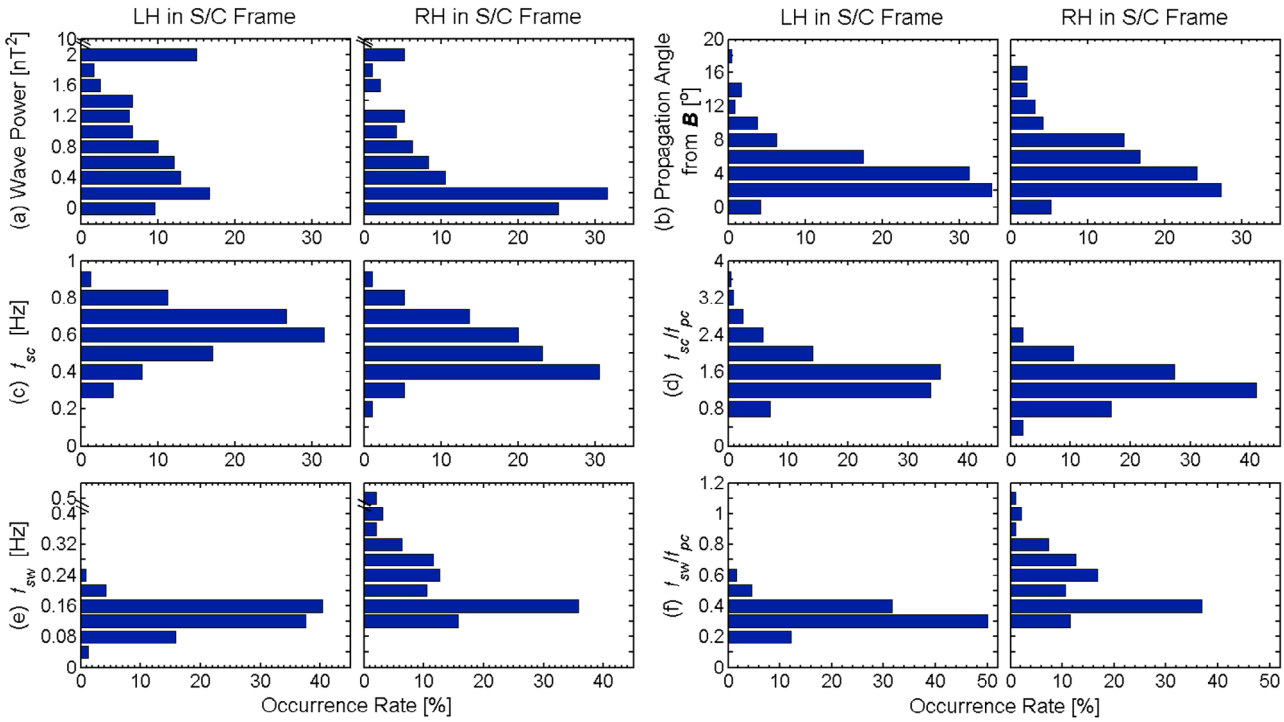

Figure 4. Comparison of the wave parameters of LH and RH waves in the spacecraft frame: (a) wave power, (b) propagation angle from $\boldsymbol{B}$ obtained using the principal axis analysis, (c) weighted frequency in the spacecraft frame f_{sc}, (d) ratio of f_{sc} to f_{pc}, indicating no simple correlation between f_{sc} and f_{pc} except that most f_{sc} are larger than f_{pc}, (e) wave frequency in the solar wind frame f_{sw}, and (f) ratio of f_{sw} to f_{pc}. The histograms of LH and RH waves are displayed in comparison for each parameter. The abscissa axis is the occurrence rate normalized by the number of LH or RH wave events. Note in the histograms of Figures 4a and 4e, the last bins used are not equally distributed as the other bins.

frequency is higher than the local f_{pc} as marked in Figure 5c. The wave has an ellipticity of −0.92 and a percentage of polarization of 95%, so it is a circularly polarized wave. It propagates 9° away from the field direction. From the hodogram in Figure 5e, we can see the wave is LH circular with respect to the minimum variance direction, which is nearly along the field direction. So the handedness is consistent with the negative ellipticity obtained from the wave analysis program.

[19] Figure 6 shows the histogram distribution of the $\boldsymbol{B}$-$\boldsymbol{R}$ angle for ICWs and the general solar wind, again indicating the waves are observed more often when the field is more radial than the background solar wind. In Figure 6b, the normalized occurrence rate in the first bin ($\boldsymbol{B}$-$\boldsymbol{R}$ angle <5°) is unexpectedly low. We suspect that this low count is due to unreliable 0° levels or the spin Doppler and attenuation effect of the spacecraft which will be elaborated later in the paper.

[20] Table 1 compares the ICWs at Helios 1 and at MESSENGER. Consistent with the higher magnetic field in 1976, the wave power and wave frequencies of ICWs from the Helios 1 survey are stronger than the ones from MESSENGER survey. Excluding data gaps of the 4 Hz magnetometer data within the 7 days, we only have data for 2.3 days. Helios 1 observed 308 ICW events, so the occurrence rate is about 136 events per day, which is significantly higher than the MESSENGER result of 27 events per day. As ICWs are not evenly observed in the solar wind, short time interval can bring large uncertainty of the occurrence rate. The discrepancy between MESSENGER and Helios 1 may represent an actual variation in occurrence rate driven by some property of the solar wind. Extensive survey and more rigorous statistical treatment are needed in the future to examine such variation and determine the representative wave properties for this heliocentric distance.

[21] For Helios 1 magnetometer data, the possible presence of "spin aliasing" of the signals by the 1 Hz rotation of the spacecraft may affect the precise determination of some ICW parameters. If spin aliasing was important, the signals rotating with the spacecraft spin and those moving opposite to the spin would be attenuated slightly differently by the antialiasing filters in the magnetometer. Then when the signals were recombined in processing to create nonspinning data, the resultant signal could have been slightly distorted. However, the similarity of the MESSENGER and Helios 1 measurements indicates that spin aliasing has not had a significant effect on the Helios 1 signals.

4. Discussion and Conclusions

[22] As listed in Table 1, our ICW observations are taken over a wide range of solar ecliptic longitude, suggesting the ICWs exist extensively and discretely in the solar wind rather than concentrated in a small longitude range. Similar to the ICWs at 1 AU, the waves near 0.3 AU are preferentially observed at small $\boldsymbol{B}$-$\boldsymbol{R}$ angle. This could be a generation or propagation effect. While the theory is not well developed for

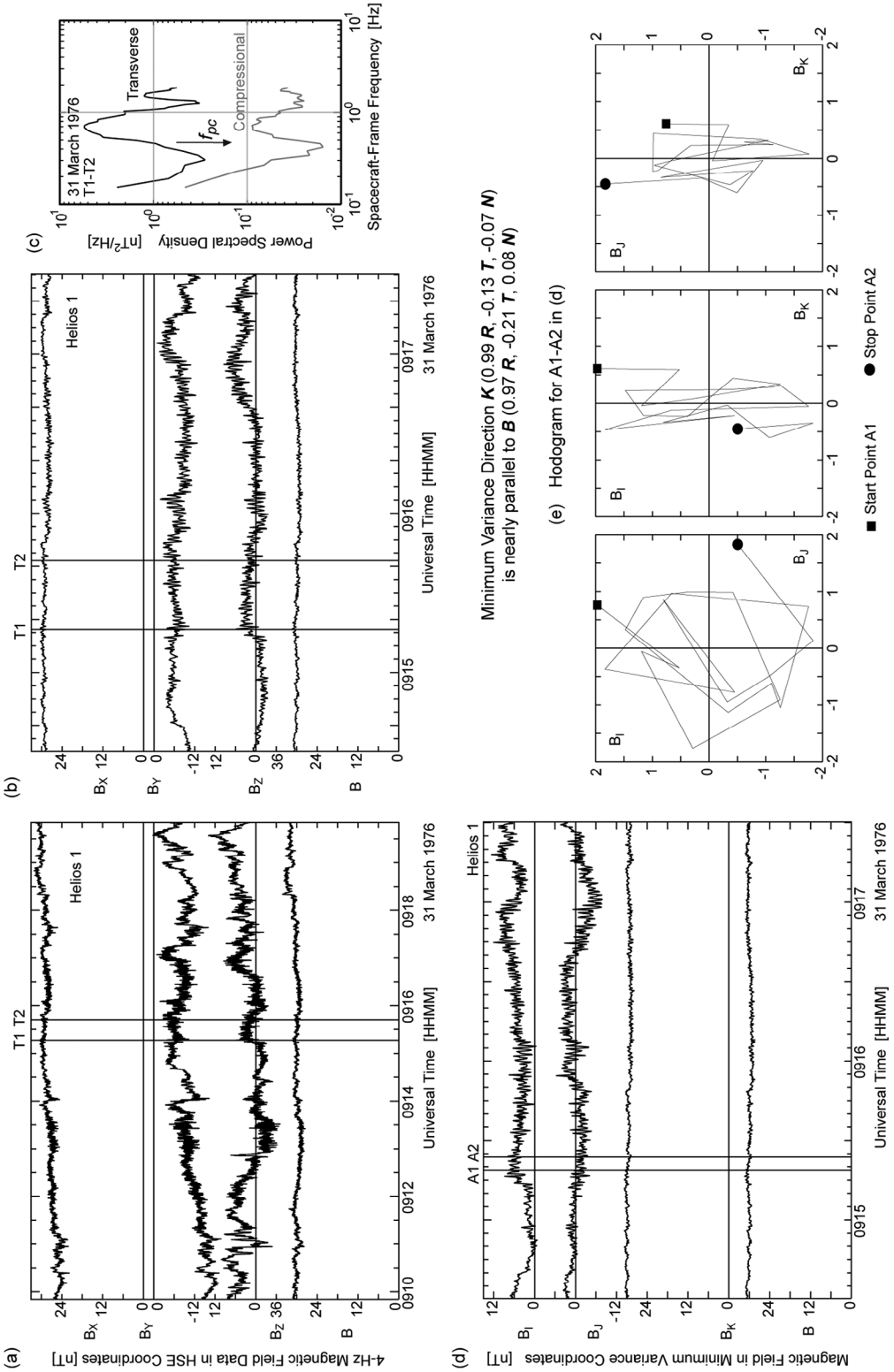

Figure 5. Example of an ICW observed by Helios 1. (a) Time series of 4 Hz magnetic field vector for 10 min in Helios solar ecliptic (HSE) coordinates, where ***X*** points toward the Sun, ***Y*** is parallel to the ecliptic plane, and ***Z*** is perpendicular to the ecliptic plane and pointing toward the north celestial pole. (b) Time series of magnetic field vector for 3 min in HSE coordinates. (c) Power spectrum of the wave during the interval T1–T2 marked in Figures 5a and 5b, averaged using five frequency bands. The transverse power is about 2 orders of magnitude stronger than the compressional power. (d) Magnetic field in the minimum variance coordinates, where the minimum variance direction ***K*** is nearly parallel to the magnetic field ***B***. (e) Hodogram for the magnetic field in the minimum variance coordinate during the time interval A1–A2 marked in Figure 5d. The wave is LH circular wave around ***K*** and ***B***.

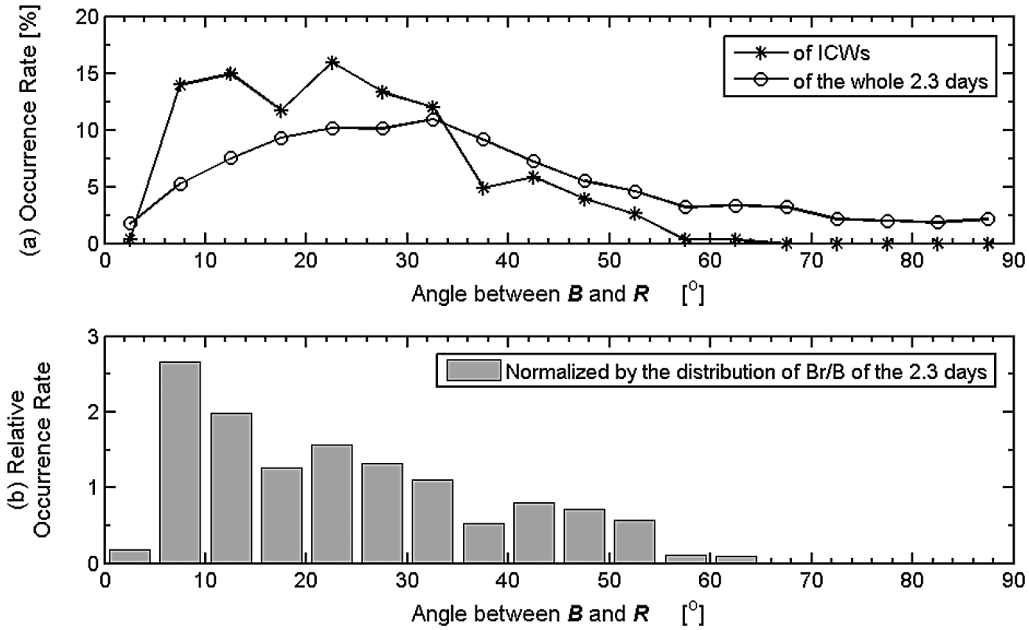

Figure 6. (a) The distributions of the ***B***-***R*** angle for ICWs observed by Helios 1 (marked by asterisk) and for the general solar wind over the 2.3 days without any data gap (marked by circle). (b) The distribution of the ***B***-***R*** angle during ICWs normalized by the ***B***-***R*** angle distribution for the solar wind.

the intermediate pickup geometry, so far theoretical studies have concluded parallel pickup ions would generate RH waves in the plasma frame at a frequency different from ICWs; therefore, the ICWs we observed are unlikely to be generated by parallel pickup ions. So the small ***B***-***R*** angle is likely due to a propagation effect. With the increase of heliocentric distance, the wave phase speed is decreasing, and the refractive index is increasing, so the wave normal direction is constantly being pulled toward the radial direction. If the IMF is not initially along the radial direction, the wave propagation angle will increase and the wave will be damped more. So only the waves of small ***B***-***R*** angle can survive due to minimal damping associated with parallel-to-***B*** propagation. Quantification of the wave refraction effect in the weakly damping media is beyond the scope of this paper and is deferred to future study.

[23] Some studies have claimed that there is possibly enough pickup He^+ in the inner heliosphere to generate the ICWs (Eberhard Möebius and George Gloeckeler, 2010, personal communication). If our waves are also associated with pickup ions of interstellar neutrals, the pickup process would produce waves similar to those found by *Murphy et al.* [1995], but our waves exhibit different characteristics from theirs; in particular, they are not well correlated with the local proton or helium cyclotron frequency (see Figure 4d) and they occur in both RH and LH polarization in the spacecraft frame. Hence, waves are being produced in both directions along the field. To the best of our knowledge, the only

Table 1. Comparison of Wave Parameters: Helios 1, MESSENGER, and STEREO Observations

Spacecraft	Helios 1	MESSENGER	STEREO A/B
Location (AU)	~0.3	~0.3	~1
Time period	25–31 March 1976 (net 2.3 days without any data gap)	31 May to 9 June 2008	A: 26 July to 2 August 2007 B: 25 July to 1 August 2007
Solar cycle phase	Solar minimum 20/21	Solar minimum 23/24	Solar minimum 23/24
Solar ecliptic longitude range (°)	229–270	33–90	A: 315–322 B: 293–299
Local field magnitude (nT)	37.6	27.1	4.3
Occurrence rate (/d)	136.6 (with large uncertainty)	33.7	15.4
Wave power (nT^2)	1.117	0.532	0.014
Relative wave amplitude normalized by background magnetic field (dB/B)	0.03	0.03	0.03
f_{sc} (Hz)	0.87	0.59	0.28
f_{sc}/f_{pc}	1.52	1.44	4.59
f_{sw} (Hz)	0.17	0.14	0.03
f_{sw}/f_{pc}	0.29	0.35	0.49
Angle between ***B*** and ***R*** (°)	22.0	18.2	25.1
Angle between ***k*** and ***R*** (°)	21.0	19.9	24.1
Propagation angle from ***B*** (°)	7.2	4.0	4.5

mechanism to do this is perpendicular pickup, where newly born ions are picked up by the solar wind onto a ring beam distribution in velocity space and are unstable to generate the ICWs. However, these waves are unlikely to be produced locally because there is no correlation with local field and also because the magnetic geometry is incorrect for this mechanism if the source is the interstellar neutrals.

[24] We can estimate the location of a distant source closer to the Sun. As mentioned earlier in the paper, if the waves were generated in the same rest frame as the spacecraft, the initial frequency should be the same as the measured f_{sc}. Taking the median f_{sc} of 0.59 Hz from the MESSENGER observations, we can derive the magnetic field in the generation region is approximately 38.7 m/q, where m/q is the mass-charge ratio normalized by protons. If the ion is He^+, the field at the generation region would be about 155 nT, and the generation location would be 0.13 AU (28 solar radii) away from the Sun. The solar wind propagation time from 0.13 to 0.3 AU is 7.3×10^4 s. As the ion cyclotron period varies with magnetic field, if we take an average cyclotron period of 4.3 s from 0.13 to 0.3 AU, the propagation time is about 1.7×10^4 ion cyclotron periods. Using 2.5-D electromagnetic hybrid simulations, *Omidi et al.* [2010] suggested such a long damping time for ICWs propagation is possible. More sophisticated simulations using the solar wind conditions are needed to verify the validity of the long damping time for the ICWs studied here.

[25] Table 1 also lists the radial variation of wave parameters from contemporary MESSENGER and STEREO observations. From 0.3 to 1 AU, the medians of the following three parameters remain nearly constant: the relative wave amplitude normalized by the background magnetic field, the ratio of f_{sw} to f_{pc}, and the wave propagation angle. On the other hand, the ICW occurrence rate decreases significantly with heliocentric distance, possibly due to the decreasing density of pickup ions and also the effect of damping. Of all the waves, 72% at 0.3 AU and 64% at 1 AU appear LH polarized in the spacecraft frame. The predominance of LH waves can be explained by the effect of propagation. After the ICWs are generated by perpendicular pickup ions, they can equally propagate parallel and antiparallel to the magnetic field. However, it takes a longer time for the inward-propagating (RH in spacecraft frame) waves to reach the spacecraft than for the outward-propagating (LH in spacecraft frame) waves. Because the RH waves are damped more due to their longer travel time, their wave power is weaker and they are harder to be detected. This is supported by the fact that the LH wave typically has a stronger wave power and a higher f_{sc} than the RH wave, as shown in Figures 4a and 4c herein and Figure 5 of *Jian et al.* [2009].

[26] While it is possible that there are some processes constantly generating ICWs throughout the inner heliosphere, it is a puzzle that we rarely see strong waves at a large $\boldsymbol{B}$-$\boldsymbol{R}$ angle as illustrated in Figure 3b, because if there is local perpendicular pickup, the large $\boldsymbol{B}$-$\boldsymbol{R}$ angle will provide large electric field for the newly born ions and should be a favorable condition for ICWs to grow. The location of the wave generation seems to be further inward than the spacecraft have gone. We recall that mirror mode waves are also seen convecting out of this region [*Russell et al.*, 2008]. These mirror mode waves can also be produced by ring beams in strong ion pickup regions such as a cometary coma [e.g., *Russell et al.*, 1987] and in the Saturnian magnetosphere beyond Enceladus [e.g., *Russell et al.*, 2006]. Similar to the mirror mode waves, the ICWs widely observed from 0.3 to 1 AU can also be treated as messengers from the regions closer to the Sun.

[27] *Gloeckler et al.* [2004] found the interstellar He ratio of the focusing cone (ecliptic longitude 173°) to other regions reached its maximum of 5.7 at 1 AU, and the ratio diminished with decreasing heliocentric distance, being about 2 at 0.1 AU. We plan to survey more ICWs at a wider range of ecliptic longitude at 1 AU to see if there is any interstellar neutral focusing cone effect and also survey the ICWs at 0.7 AU to better examine the radial variation. As the wave generation mechanism needs to meet the observed wave properties and a reasonable damping time for the ICWs, coordinated theoretical and modeling work on both ICW generation and propagation is needed to determine an appropriate generation scenario. Because the waves we observed within 1 AU have different features from the waves at 5 AU generated by locally pickup ions, to fully understand these waves, we will need to send spacecraft much closer to the Sun with the needed plasma and electric and magnetic field instruments to help solve this mystery.

[28] **Acknowledgments.** This work is supported by NASA's STEREO program through grant NAS5-03131 administered by University of California-Berkeley. We thank all the PIs for making the data available. We appreciate Fritz Neubauer, Peter Gary, and Philip Isenberg for their useful discussions.

[29] Philippa Browning thanks Nick Omidi and another reviewer for their assistance in evaluating this manuscript.

References

Anderson, B. J., M. H. Acuña, D. A. Lohr, J. Scheifele, A. Raval, H. Korth, and J. A. Slavin (2007), The magnetometer instrument on MESSENGER, *Space Sci. Rev.*, *131*, 417–450.

Blanco-Cano, X. G. (1995), Waves and particles upstream of Earth's bow shock, Ph.D. thesis, Univ. of London, London, U. K.

Domingue, D. L., and C. T. Russell (Eds.) (2007), *The MESSENGER Mission to Mercury*, 624 pp., *Space Sci. Rev.*, vol. 131, Springer, Netherlands.

Fraser, B. J. (1985), Observations of ion cyclotron waves near synchronous orbit and on the ground, *Space Sci. Rev.*, *42*, 357–374.

Geiss, J., G. Gloeckler, U. Mall, R. von Steiger, A. B. Galvin, and K. W. Ogilvie (1994), Interstellar oxygen, nitrogen, and neon in the heliosphere, *Astron. Astrophys.*, *282*, 924–933.

Gloeckler, G., A. B. Galvin, F. M. Ipavich, J. Geiss, H. Balsiger, R. von Steiger, L. A. Fisk, K. W. Ogilvie, and B. Wilken (1993), Detection of interstellar pick-up hydrogen in the solar system, *Science*, *261*, 70–73.

Gloeckler, G., et al. (2004), Observations of the helium focusing cone with pickup ions, *Astron. Astrophys.*, *426*, 845–854.

Huddleston, D. E., R. J. Strangeway, J. Warnecke, C. T. Russell, and M. G. Kivelson (1998), Ion cyclotron waves in the Io torus: Wave dispersion, free energy analysis, and SO_2^+ source rate estimates, *J. Geophys. Res.*, *103*(E9), 19,887–19,899, doi:10.1029/97JE03557.

Isenberg, P. A. (1996), Effects of spatial transport and ambient wave intensity on the generation of MHD waves by interstellar pickup protons, in *Proceedings of the Eighth International Solar Wind Conference: Solar Wind Eight*, *Am. Inst. Phys.*, vol. 382, edited by D. Winterhalter et al., pp. 626–629, AIP Press, Woodbury, N. Y.

Jian, L. K., C. T. Russell, J. G. Luhmann, R. J. Strangeway, J. S. Leisner, and A. B. Galvin (2009), Ion cyclotron waves in the solar wind observed by STEREO near 1 AU, *Astrophys. J.*, *701*, L105.

Lacombe, C., E. Kinzelin, C. C. Harvey, D. Hubert, A. Mangeney, J. Elaoufir, D. Burgess, and C. T. Russell (1990), Nature of turbulence observed by ISEE 1-2 during a quasi-perpendicular crossing of the Earth's bow shock, *Ann. Geophys.*, *8*, 489–502.

Lee, M. A., and W.-H. Ip (1987), Hydromagnetic wave excitation by ionized interstellar hydrogen and helium in the solar wind, *J. Geophys. Res.*, *92*(A10), 11,041–11,052, doi:10.1029/JA092iA10p11041.

Leisner, J. S., C. T. Russell, M. K. Dougherty, X. Blanco-Cano, R. J. Strangeway, and C. Bertucci (2006), Ion cyclotron waves in Saturn's E ring: Initial Cassini observations, *Geophys. Res. Lett.*, *33*, L11101, doi:10.1029/2005GL024875.

Li, X., S. R. Habbal, J. V. Hollweg, and R. Esser (1999), Heating and cooling of protons by turbulence-driven ion cyclotron waves in the fast solar wind, *J. Geophys. Res.*, *104*(A2), 2521–2535, doi:10.1029/1998JA900126.

Means, J. D. (1972), Use of the three-dimensional covariance matrix in analyzing the polarization properties of plane waves, *J. Geophys. Res.*, *77*(28), 5551–5559, doi:10.1029/JA077i028p05551.

Möbius, E., D. Hovestadt, B. Klecker, M. Scholer, G. Gloecker, and F. M. Ipavich (1985), Direct observation of He^+ pick-up ions of interstellar origin in the solar wind, *Nature*, *318*, 426–429.

Murphy, N., E. J. Smith, B. T. Tsurutani, A. Balogh, and D. J. Southwood (1995), Further studies of waves accompanying the solar wind pick-up of interstellar hydrogen, *Space Sci. Rev.*, *72*, 447–452.

Murphy, N., E. J. Smith, J. Wolf, and D. S. Intriligator (1998), A reexamination of "interstellar ion waves" previously identified in Pioneer 10 magnetic field data, *Geophys. Res. Lett.*, *25*(19), 3721–3724, doi:10.1029/98GL02802.

Neubauer, F. M., G. Musmann, and G. Dehmel (1977), Fast magnetic fluctuations in the solar wind: Helios 1, *J. Geophys. Res.*, *82*(22), 3201–3212, doi:10.1029/JA082i022p03201.

Neubauer, F. M., K.-H. Glassmeier, A. J. Coates, and A. D. Johnstone (1993), Low-frequency electromagnetic plasma waves at comet P/Grigg-Skjellerup: Analysis and interpretation, *J. Geophys. Res.*, *98*(A12), 20,937–20,953, doi:10.1029/93JA02532.

Omidi, N., R. Thorne, and J. Bortnik (2010), Nonlinear evolution of EMIC waves in a uniform magnetic field: 1. Hybrid simulations, *J. Geophys. Res.*, *115*, A12241, doi:10.1029/2010JA015607.

Russell, C. T., and X. Blanco-Cano (2007), Ion-cyclotron wave generation by planetary ion pickup, *J. Atmos. Sol.-Terr. Phys.*, *69*, 1723–1738.

Russell, C. T., W. Riedler, K. Schwingenschuh, and Y. Yeroshenko (1987), Mirror instability in the magnetosphere of comet Halley, *Geophys. Res. Lett.*, *14*(6), 644–647, doi:10.1029/GL014i006p00644.

Russell, C. T., J. S. Leisner, C. S. Arridge, M. K. Dougherty, and X. Blanco-Cano (2006), Nature of magnetic fluctuations in Saturn's middle magnetosphere, *J. Geophys. Res.*, *111*, A12205, doi:10.1029/2006JA011921.

Russell, C. T., L. K. Jian, J. G. Luhmann, T. L. Zhang, F. M. Neubauer, R. M. Skoug, X. Blanco-Cano, N. Omidi, and M. M. Cowee (2008), Mirror mode waves: Messengers from the coronal heating region, *Geophys. Res. Lett.*, *35*, L15101, doi:10.1029/2008GL034096.

Stix, T. H. (1962), *The Theory of Plasma Waves*, McGraw-Hill, New York.

Tu, C.-Y., and E. Marsch (2001), On cyclotron wave heating and acceleration of solar wind ions in the outer corona, *J. Geophys. Res.*, *106*(A5), 8233–8252, doi:10.1029/2000JA000024.

Williams, L. L., and G. P. Zank (1994), Effect of magnetic field geometry on the wave signature of the pickup of interstellar neutrals, *J. Geophys. Res.*, *99*(A10), 19,229–19,244, doi:10.1029/94JA01657.

Wu, C. S., and R. C. Davidson (1972), Electromagnetic instabilities produced by neutral-particle ionization in interplanetary space, *J. Geophys. Res.*, *77*(28), 5399–5406, doi:10.1029/JA077i028p05399.

Wu, C. S., R. E. Hartle, and K. W. Ogilvie (1973), Interaction of singly charged interstellar helium ions with the solar wind, *J. Geophys. Res.*, *78*(1), 306–309, doi:10.1029/JA078i001p00306.

B. J. Anderson, Applied Physics Laboratory, Johns Hopkins University, Baltimore, MD 20723, USA.

S. A. Boardsen, Heliophysics Science Division, NASA Goddard Space Flight Center, Greenbelt, MD 20771, USA.

M. M. Cowee, Space Science and Applications (ISR-1), Los Alamos National Laboratory, Los Alamos, NM 87545, USA.

L. K. Jian, C. T. Russell, and R. J. Strangeway, Institute of Geophysics and Planetary Physics, University of California, Los Angeles, CA 90095, USA. (jlan@igpp.ucla.edu)

J. G. Luhmann, Space Science Laboratory, University of California, Berkeley, CA 94720, USA.

A. Wennmacher, Institute of Geophysics and Meteorology, University of Cologne, Cologne, D-50923, Germany.